



## Determination of cost optimal operating conditions for decoloration and mineralization of C. I. Reactive Blue 268 by UV/H<sub>2</sub>O<sub>2</sub> process

Nina Novak<sup>a,\*</sup>, Alenka Majcen Le Marechal<sup>a</sup>, Miloš Bogataj<sup>b</sup>

<sup>a</sup> Faculty of Mechanical Engineering, University of Maribor, Smetanova ulica 17, SI-2000 Maribor, Slovenia

<sup>b</sup> Faculty of Chemistry and Chemical Engineering, University of Maribor, Smetanova ulica 17, SI-2000 Maribor, Slovenia

### ARTICLE INFO

#### Article history:

Received 2 October 2008

Received in revised form 3 January 2009

Accepted 22 February 2009

#### Keywords:

Wastewater treatment

Textile dyes

Response surface methodology

Mathematical programming

Process optimization

### ABSTRACT

The UV/H<sub>2</sub>O<sub>2</sub> process has often been proposed as an effective treatment technology for remediation of colored wastewaters. However, it has frequently been noted that it is not as economically efficient as other treatment technologies. To limit this drawback as much as possible, an effort to optimize the treatment technology from both the economical and operating points of view is needed.

This paper presents a study on determination of cost optimal operating conditions for decoloration and mineralization of C. I. Reactive Blue 268 by the UV/H<sub>2</sub>O<sub>2</sub> process. Dye concentration, hydrogen peroxide concentration, pH, treatment time, and temperature were considered to be influential operating parameters. Cost of electricity, cost of hydrogen peroxide, and cost of water needed to adjust the dye concentration were considered to be relevant operating costs.

The presented approach is based on response surface methodology in conjunction with mathematical programming. The results obtained clearly indicate that, in order to assure effective and economically efficient operation, the UV/H<sub>2</sub>O<sub>2</sub> process should be simultaneously optimized from the perspective of both operational and economic efficiency.

© 2009 Elsevier B.V. All rights reserved.

### 1. Introduction

Substantial effort has been devoted to developing technologies that would reduce the negative impact of colored wastewaters on the environment. The most interesting are technologies that transform hazardous and toxic pollutants into environmentally friendly compounds. For this reason, Advanced Oxidation Processes (AOPs) have attracted considerable attention, and numerous studies on their ability to degrade colored compounds in wastewaters are reported in the literature [1–5].

Among the AOPs, the UV/H<sub>2</sub>O<sub>2</sub> process was believed to be one of the most promising treatment technologies, as no sludge is formed during the treatment. However, in comparison to conventional treatment technologies, the UV/H<sub>2</sub>O<sub>2</sub> technology is relatively expensive. It consumes large quantities of electrical energy needed for generation of UV radiation, and its consumption, without doubt, represents the major fraction of operating costs. Furthermore, the costs related to the consumption of H<sub>2</sub>O<sub>2</sub> are not negligible [6].

Consequently, researchers are aware that to offer a technology that is viable from an industrial applicability point of view, the

UV/H<sub>2</sub>O<sub>2</sub> process needs to be optimized. Various techniques have been employed to find optimal operating conditions. Abdullah et al. [7] optimized the UV/H<sub>2</sub>O<sub>2</sub> performance (decoloration of C. I. Natural Red 4) through a systematic search for the most promising operating conditions by first varying the dye and H<sub>2</sub>O<sub>2</sub> concentration. After their optimal concentrations were established, the effects of pH and various ions on the process efficiency were studied. Shu et al. [8] optimized the C. I. Acid Black 1 decoloration process through an inspection of the generated plots of electric power consumption and retention time as functions of the operating parameters. Guimarães et al. [9] optimized the operating parameters for the C. I. Acid Brown 75 decoloration using neural networks. Their approach is based on a determination of the maximum amount of H<sub>2</sub>O<sub>2</sub> to be added in order to achieve the desired decoloration level in the least amount of time. Recently, Körbahti and Rauf [10] and Rauf et al. [11] utilized the response surface methodology (RSM) to optimize the decoloration of C. I. Acid Red 94 and C. I. Basic Red 2, respectively. The authors considered initial dye concentration, initial H<sub>2</sub>O<sub>2</sub> concentration, and pH as influential operating conditions. These are outstanding scientific contributions, however, the authors focused almost exclusively on finding optimal operating conditions with no or very little consideration of the accompanying operating costs.

Another issue that has been often overlooked in optimization of technologies for colored wastewater treatment [12–14] is that

\* Corresponding author. Tel.: +386 2 220 7910; fax: +386 2 220 7990.  
E-mail address: [nina.novak@uni-mb.si](mailto:nina.novak@uni-mb.si) (N. Novak).

### Nomenclature

$A$	absorbance (/)
$\Delta A$	decoloration at $\lambda_{\max}$ (%)
$c$	molar concentration (mmol/L)
$C$	cost, price ( $\epsilon$ , $\epsilon$ /quantity)
$I$	photonic flux ( $\mu\text{Einstein/s}$ )
$N$	number (/)
$P$	power (kW)
SAC	spectral absorption coefficient ( $\text{m}^{-1}$ )
$t$	time (min)
$T$	temperature ( $^{\circ}\text{C}$ )
TOC	total organic carbon (mg/L)
$V$	volume (L)
$w$	mass fraction (/ , %)

### Greek symbols

$\gamma$	mass concentration (mg/L)
$\lambda$	wavelength (nm)
$\rho$	density (kg/L)

### Subscripts/superscripts

E	electricity
f	final
i	initial
L	loadings
R	reactor
T	total

some independent variables are often found to be more or less fixed in a certain way. For example, consider the dye concentration in wastewater to be treated in an end-of-pipe treatment process. Its concentration can be manipulated, for example, by changes in operating conditions of the preceding process operations, replacement of the existing equipment with different – potentially more efficient – technology, or by either concentrating or diluting the discharge stream. And even though some of these possibilities may readily be available to implement, each of them carries inherent costs associated with investment and operation. Evidently, such costs should be considered in the search for the optimal solution.

In this work, decoloration and mineralization of C. I. Reactive Blue 268 using UV/H<sub>2</sub>O<sub>2</sub> treatment technology was investigated. The dye is used for cellulose fibers dyeing, and belongs to a class of triphenodioxazine dyes, which combine the advantages of azo and anthraquinone dyes. As such, it is characterized by good fastness properties, brightness [15], and high stability to photo-reduction [16]. The decoloration and mineralization process was simultaneously optimized from the perspective of operational and economic efficiency. The proposed optimization approach combines response surface methodology and mathematical programming.

## 2. Optimization methodology

As denoted in the introduction, the proposed optimization approach combines the response surface methodology and mathematical programming. Flowchart in Fig. 1 represents the activities within the framework of the proposed approach. After the prescreening (preliminary experimentation), an appropriate experimental design is selected, the experiments are performed, and the results are analyzed (modeling of responses, statistical analyses). If statistical tests regarding the obtained response models (polynomial approximations) produce unsatisfactory results, modifications in response surface modeling and/or experimental design are required. If the statistics is satisfactory, the obtained response models are used to formulate an appropriate optimization problem, which is solved using a software for constrained optimization.

In this work, it is assumed that the responses are modeled by estimating the coefficients of the second-order model, given by:

$$y = \beta_0 + \sum_{j=1}^l \beta_j x_j + \sum_{j=1}^l \beta_{jj} x_j^2 + \sum_{j,k} \beta_{jk} x_j x_k + \varepsilon \quad (1)$$

In Eq. (1),  $y$  is the measured response,  $x_j$  and  $x_k$  are the independent variables,  $\beta_j$ ,  $\beta_{jj}$  and  $\beta_{jk}$  are the model coefficients, and  $\varepsilon$  is the error. The polynomial function (Eq. (1)) is an approximation of the true response function for a given response over the entire range of independent variables. If the range is restricted to a relatively small region, the approximation is usually in good agreement with the true response function [17] and can be used in analysis, simulation, and optimization etc. of the process.

Finding optimal operating conditions for a given process using the response surface methodology translates to finding a set of independent variables that minimize or maximize the responses

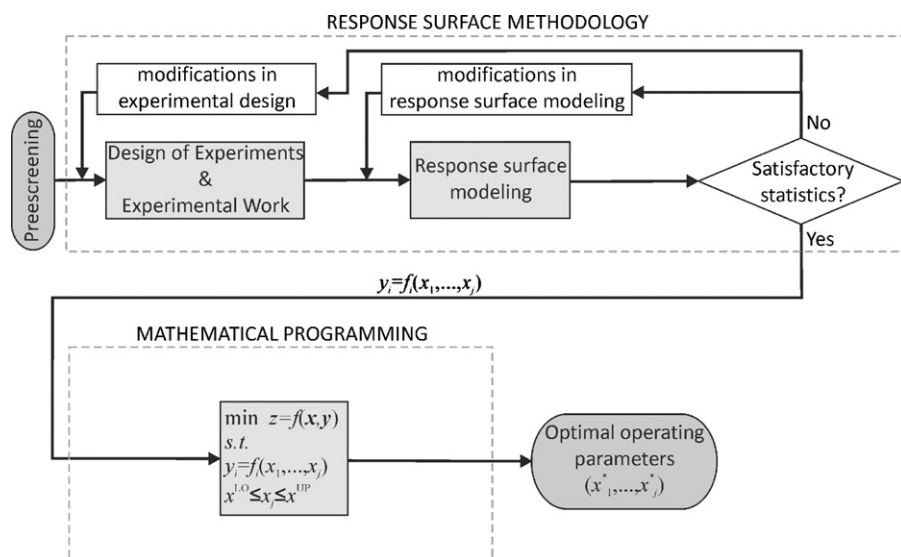


Fig. 1. Process optimization strategy combining response surface methodology and mathematical programming.

predicted by the polynomial approximation. In general, the simultaneous optimization of multiple responses predicted by the second-order models is considered to be a nonlinear multiobjective optimization problem [18,19]. For a comprehensive review of the methods used in solving these problems the reader is referred to Miettinen [20]. However, when the responses are not conflicting and their attainable values are well-scaled, the following monoobjective mathematical program (2) can be assumed as a fairly reasonable approach. In the remainder of the paper we will refer to it as response maximization (RM) formulation.

$$\begin{aligned} \max \quad & z = \sum_{i=1}^k \pm y_i \\ \text{s.t.} \quad & \\ & y_i = \beta_{i0} + \sum_{j=1}^l \beta_{ij}x_j + \sum_{j=1}^l \beta_{ijj}x_j^2 + \sum_{j<k}^l \sum \beta_{ijk}x_jx_k + \varepsilon_i \\ & x_j^{\text{LO}} \leq x_j \leq x_j^{\text{UP}} \end{aligned} \quad (2)$$

The objective function is a sum of  $k$  responses. The responses to be maximized have a positive sign, while a negative sign is assigned to the responses that are to be minimized. Independent variables  $x_j$  are constrained by their experimental lower and upper bounds  $x_j^{\text{LO}}$  and  $x_j^{\text{UP}}$ , respectively. The solution to RM is a set of independent variables ( $x_1^*$ ,  $x_2^*$ , ...,  $x_j^*$ ) that give minimum/maximum responses,  $y_i$ .

In many engineering applications, however, the responses only need to satisfy certain threshold limits, which may not necessarily coincide with the attainable extreme values of the responses. In addition, attaining these extreme values can cause the operating costs to become unacceptably high, making the process economically inefficient. In such cases, a trade-off between the economic efficiency and the performance of a given process should be taken into consideration.

For the above reason, an approach to optimize the process performance (modeled by second-order approximating functions) by minimizing the relevant operating costs of the process, as opposed to finding the attainable extremes of the responses, is proposed. To accomplish this task, the RM is reformulated. The obtained mathematical program (3) will be referred to as cost minimization (CM) formulation.

$$\begin{aligned} \min \quad & C = \sum_{m=1}^n C_m \\ \text{s.t.} \quad & \\ & y_i = \beta_{i0} + \sum_{j=1}^l \beta_{ij}x_j + \sum_{j=1}^l \beta_{ijj}x_j^2 + \sum_{j<k}^l \sum \beta_{ijk}x_jx_k + \varepsilon_i \\ & C_m = f_m(x_1, x_2, \dots, x_j) \\ & y_i (\leq \geq) y_i^{\text{TL}} \\ & x_j^{\text{LO}} \leq x_j \leq x_j^{\text{UP}} \end{aligned} \quad (3)$$

In contrast to RM, the objective function in CM is a sum of  $n$  operating costs, defined as functions of independent variables  $f_m(x_1, x_2, \dots, x_j)$ . The desired efficiency is attained by constraining the responses through inequalities, stating that a given response should be greater than or equal to, or less than or equal to a predetermined threshold limit  $y_i^{\text{TL}}$ .

### 2.1. Remarks on the optimization methodology

The proposed approach utilizes the advantages of response surface methodology and mathematical programming.

- Response surface methodology is a powerful tool for deriving empirical correlations among operating conditions and responses if the corresponding system of analytical functions is unknown and/or very hard to derive. Yet, the researcher should be aware that the response surface models are only approximations of the true response functions, and also case-specific. If there exists a doubt in their quality (i.e. poor prediction properties), they should not be used.
- Mathematical programming enables incorporation of explicit cost functions, which correlate operating parameters to their costs. Therefore, a given process can be optimized not only from the perspective of its performance, but also from the perspective of economic efficiency. Optimization problems can be formulated in many different ways, depending on the goals to be achieved. There is no general guidance on this topic. However, the researcher should carefully derive additional functions, if any. Often some simplifying case-specific assumptions are needed. They too should be carefully dealt with in order to avoid wrong or misleading conclusions. It should also be noted that the optimization problems, as given by Eqs. (2) and (3), are nonlinear and nonconvex. For this reason, unless special techniques for global optimization are used, the solutions obtained are not necessarily globally optimal.

## 3. Experimental

### 3.1. Photo-reactor set-up

Photo-oxidation experiments were performed in a batch reactor (Helios ItalQuartz) with a maximum working volume of 1.8 L. The source of UV radiation was a medium pressure Hg lamp operating at 500 W. The incident photonic flux was measured by hydrogen peroxide actinometry according to Nicole et al. [21] ( $I_0 = 6.0 \pm 0.1 \mu\text{Einstein/s}$ ). The photo-reactor set-up is schematically presented in Fig. 2.

To keep the temperature of the dye solutions during the experiments constant, the reactor was cooled using two coolants; air and cooling water. The purpose of air-cooling was to facilitate the dissipation of heat flux produced by the UV lamp to the extent at which the dye solution temperature could be controlled solely by the adjustments of the cooling water inlet temperature. Air inlet temperature and volumetric flow rate, as well as the cooling water flow rate, were constant in all the experiments.

As shown in Fig. 2, of the two coolants, only the air is in direct contact with the surface of the UV lamp. As such, it has potentially greater impact on the operating temperature of the UV lamp than the cooling water, which is contained in a quartz cooling jacket physically separated from the surface of the UV lamp. Keeping the air flow rate and inlet temperature constant should guarantee a relatively constant temperature of air in the direct vicinity of the UV lamp's walls, consequently assuring its constant operating temperature and efficiency.

Although the efficiency of medium pressure Hg lamps is rather insensitive to the changes in operating temperature [22], the above precautionary measure was taken to minimize the eventual fluctuations in its efficiency caused by cooling.

### 3.2. Experimental design

In this study, a face centered central composite design (CCD) comprising five independent variables was chosen. In total, 50 experimental runs were conducted. To provide good variance of prediction, eight center points were used. Initial dye concentration, initial  $\text{H}_2\text{O}_2$  concentration, pH, temperature, and treatment time were selected as independent variables. Their ranges are presented

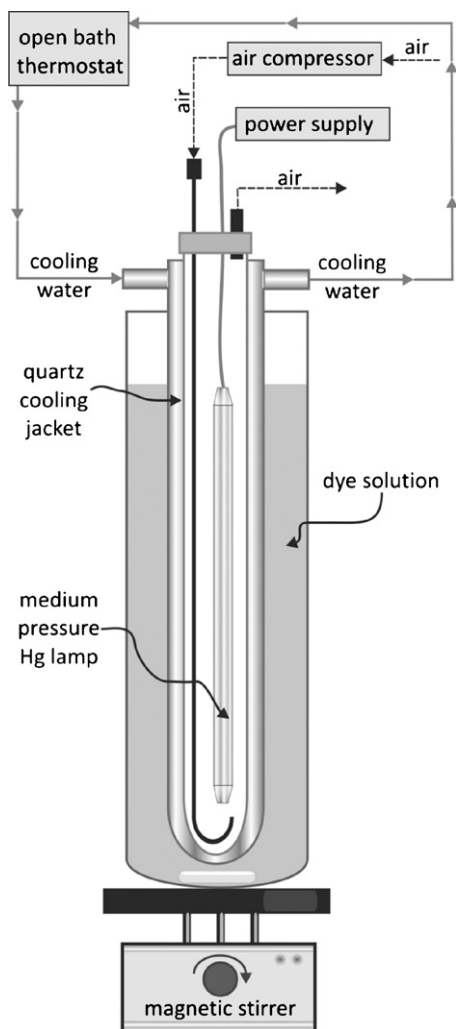


Fig. 2. Photo-reactor set-up.

in actual values in Table 1. A brief discussion on how and why the ranges were chosen as such is given in the following paragraph.

Commonly, the wastewater obtained after reactive dyeing of cellulose fibers is alkaline [15]. For this reason, the pH at the high level was set to 11. On the other hand, according to the literature [23,24], the UV/H<sub>2</sub>O<sub>2</sub> treatment technology is more efficient in weakly acidic and neutral than in alkaline conditions. Therefore, a part of acidic pH region was also explored.

The concentration of the dye remaining in the colored textile wastewaters depends mostly on the chemical structure of the dye and the type of the dyeing process (exhaustion dyeing, pad dyeing). Also, often the dye-bath effluents are mixed with rinsing water, which lowers the dye concentrations. The dye used in this work belongs to a group of high-fixation poly-functional reactive dyestuffs for exhaustion dyeing of cellulosic fibers [25]. In addition, high fixation, which leads to a significant reduction in the amount of dye lost to the effluent, is also guaranteed by the manufacturer

**Table 1**  
Levels of independent variables.

Independent variable	Low level	Medium level	High level
$\gamma_{\text{Dye}}$ (mg/L)	10	45	80
$c_{\text{H}_2\text{O}_2}$ (mmol/L)	5	102.5	200
pH (/)	5.5	8.25	11
$T$ (°C)	20	27.5	35
$t$ (min)	10	35	60

(Ciba Specialty Chemicals). Although, the reported dye concentrations found in the dyehouse wastewaters range from 5 to 1500 mg/L [26], the preceding statements make the selected dye concentration range credible for the purposes of this study.

Temperature range was bounded by the capability of laboratory equipment to maintain constant temperature throughout the experiments. Treatment time and hydrogen peroxide concentration ranges were chosen on the basis of preliminary testing.

As dependent variables, responses, percent of decoloration ( $\Delta A$ ) at  $\lambda_{\text{max}}$ , three spectral absorption coefficients ( $\text{SAC}_{\lambda = 436 \text{ nm}}$ ,  $\text{SAC}_{\lambda = 525 \text{ nm}}$ ,  $\text{SAC}_{\lambda = 620 \text{ nm}}$ ), and total organic carbon (TOC), were considered.

### 3.3. Chemicals

A commercial reactive triphenodioxazine dye C. I. Reactive Blue 268 (Cibacron Brilliant Blue FN-G, CAS No. 163062-28-0) manufactured by Ciba Specialty Chemicals was used without further purification (70–80% purity approximately). Its chemical structure was not disclosed by the manufacturer.

Hydrogen peroxide solution ( $w = 30\%$ , with  $\rho = 1.11 \text{ g/mL}$ ) of analytical grade was obtained from Belinka. Adjustment of pH was conducted using H<sub>2</sub>SO<sub>4</sub> ( $\rho = 1.84 \text{ g/mL}$ ) from Merck and NaOH from Fluka. All the solutions were prepared with deionized water ( $\chi = 1.2 \mu\text{S/cm}$ ).

### 3.4. Photochemical experiments

A stock solution of the dye was prepared by dissolving 2.5 g of the dye in 1 L of deionized water. After pH adjustment to 11.0, the solution was heated to 60 °C, and maintained for 4 h to allow complete hydrolysis, since reactive dyes are found in wastewater in the hydrolyzed form. The necessary dilutions of this stock solution were prepared with deionized water.

During each run, the reactor was filled with aqueous dye solution and stirred with a magnetic stirrer. The required temperature and pH were adjusted, and the specified volume of H<sub>2</sub>O<sub>2</sub> was added. The reaction started when the lamp was switched on.

### 3.5. Analytical methods

Samples were collected before and after the reaction. The absorption spectra were recorded on a 8453 UV–VIS spectrophotometer (Agilent) over the range 400–800 nm. The absorbance was registered at the peak wavelength, which for the selected dye corresponds to  $\lambda_{\text{max}} = 634 \text{ nm}$ , and at three standard wavelengths according to the Slovenian environmental regulations [27]:  $\lambda_1 = 436 \text{ nm}$ ,  $\lambda_2 = 525 \text{ nm}$ , and  $\lambda_3 = 620 \text{ nm}$ .

Decoloration of the dye solution was assessed by the spectral absorption coefficients, and percentage decrease in absorbance at the peak wavelength. The spectral absorption coefficients at the above-documented wavelengths are common indicators for the coloration of waters. They are defined as:

$$\text{SAC}_{\lambda} (\text{m}^{-1}) = \frac{1}{l} A_{\lambda} \quad (4)$$

where  $l$  (m) is the optical length.

Percentage decrease in absorbance was calculated using Eq. (5).

$$\Delta A (\%) = 100 \left( \frac{A_i - A_f}{A_i} \right) \quad (5)$$

where  $A_f$  and  $A_i$  are the final and initial values of absorbance at peak wavelength.

The extent of mineralization of the reaction samples was monitored by measuring the total organic carbon using DC-190 analyzer (Dohrmann).

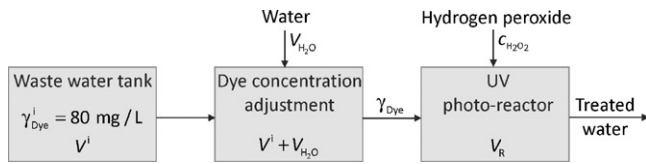


Fig. 3. Schematic representation of the treatment process.

## 4. Results

### 4.1. Problem statement

The RM and CM formulations are generalized formulations, which become unique optimization problems once the case-specific polynomial approximating functions, cost functions, and limits on the responses are derived. Among these, especially the cost functions and the limits on the responses depend on how the optimization problem is postulated. In this work, the problem statement is given as follows.

Wastewater of volume  $V^i$ , containing dye C. I. Reactive Blue 268 of concentration  $\gamma_{Dye}^i = 80 \text{ mg/L}$  is to be treated using UV/ $H_2O_2$  treatment technology. The treatment is conducted in a photo-reactor of volume  $V_R$ . Prior the treatment, as depicted in Fig. 3, the dye concentration can be adjusted by dilution with water of volume  $V_{H_2O}$ . The objective is to simultaneously determine the operating conditions (independent variables presented in Table 1), such that the legislation limits on environmental parameters (responses) are satisfied, and relevant operating costs are minimized.

In addition, the following case-specific assumptions are used:

- The initial volume of the wastewater equals the volume of the photo-reactor ( $V^i = V_R = 1.8 \text{ L}$ ).
- A single reactor is used and the process operates in a batch mode.
- Costs of electricity, hydrogen peroxide, and water used for dilution are the relevant costs to be minimized.
- The costs that arise due to pH adjustments and temperature control are neglected as they were determined to be several orders of magnitude smaller than the total treatment costs.
- The volume of added hydrogen peroxide does not affect the total volume of the dye solution as it is expected to be several orders of magnitude smaller than the volume of the solution to be treated.
- In case of a partially filled reactor, the UV radiation is not utilized to the full extent because the UV lamp is not completely immersed in solution (Fig. 2). Therefore, the treatment time of a partially filled reactor exceeds the treatment time of a fully filled reactor.

### 4.2. Mathematical program (CM formulation)

Taking into consideration the problem statement and the above assumptions, the following mathematical program (Eqs. (6)–(24)) is derived:

$$\min C_T = \frac{P_{UV}t}{60} C_E N_L + \frac{c_{H_2O_2} M_{H_2O_2} (V^i + V_{H_2O})}{1000 \rho_{H_2O_2} w_{H_2O_2}} C_{H_2O_2} + V_{H_2O} C_{H_2O} \quad (6)$$

where  $C_T$  is the total treatment cost,  $P_{UV}$  is the power of the UV lamp,  $t$  is the treatment time of a single batch,  $N_L$  is the number of reactor loadings.  $c_{H_2O_2}$ ,  $M_{H_2O_2}$ , and  $w_{H_2O_2}$  are the concentration, molar mass and mass fraction of hydrogen peroxide, and  $\rho_{H_2O_2}$  is the density of the hydrogen peroxide solution.  $V^i$  is the initial volume of the dye solution (see assumption “a”), and  $V_{H_2O}$  is the volume of water utilized for the dilution.  $C_E$ ,  $C_{H_2O_2}$ , and  $C_{H_2O}$  are the prices of electricity, hydrogen peroxide and water.

Objective function (Eq. (6)) to be minimized is nonlinear and comprises three cost terms. The first term accounts for the electricity cost. Note that the time ( $t$ ) corresponds to the treatment time of a single batch. Therefore, because total treatment costs are to be minimized, multiplication by a number of reactor loadings ( $N_L$ ) is necessary. Costs of hydrogen peroxide and water are correlated through the second and third terms, respectively. Division of the first term by 60, and the second term by 1000 is needed to make the equation dimensionally consistent.

Eqs. (7)–(11) represent second-order approximating functions of each response monitored. They were obtained by analysis of the experimental results using a commercially available software package Design Expert (Stat-Ease Inc.). Review of statistical information regarding the polynomial approximations and various diagnostic plots available in Design Expert software showed that the response models can be used to navigate the design space. Some of the relevant statistical data are presented in Appendix A.

$$\begin{aligned} \sqrt{\Delta A} = & -4.312 - 0.058\gamma_{Dye} + 0.024c_{H_2O_2} + 0.058t + 3.828\text{pH} \\ & + 2.151 \times 10^{-4}\gamma_{Dye}c_{H_2O_2} + 2.840 \times 10^{-4}\gamma_{Dye}t \\ & - 1.330 \times 10^{-4}c_{H_2O_2}t - 3.595 \times 10^{-3}c_{H_2O_2}\text{pH} \\ & + 8.090 \times 10^{-3}t\text{pH} - 1.047 \times 10^{-3}(t)^2 - 0.74(\text{pH})^2 \quad (7) \end{aligned}$$

$$\begin{aligned} \log(\text{SAC}_{\lambda=436\text{nm}}) = & -5.039 + 0.018\gamma_{Dye} + 0.015c_{H_2O_2} \\ & + 0.398T + 0.015t - 3.548 \times 10^{-5}\gamma_{Dye}c_{H_2O_2} \\ & + 7.779 \times 10^{-5}(c_{H_2O_2})^2 - 7.408 \times 10^{-3}(T)^2 \\ & - 3.318 \times 10^{-4}(t)^2 \quad (8) \end{aligned}$$

$$\begin{aligned} \log(\text{SAC}_{\lambda=525\text{nm}}) = & -7.848 + 0.024\gamma_{Dye} - 0.020c_{H_2O_2} + 0.561T \\ & - 0.010t + 0.132\text{pH} - 5.818 \times 10^{-5}\gamma_{Dye}c_{H_2O_2} \\ & + 1.054 \times 10^{-4}(c_{H_2O_2})^2 - 0.010(T)^2 \quad (9) \end{aligned}$$

$$\begin{aligned} \log(\text{SAC}_{\lambda=620\text{nm}}) = & -6.070 + 0.029\gamma_{Dye} - 0.032c_{H_2O_2} + 0.440T \\ & - 0.016t + 0.147\text{pH} - 7.582 \times 10^{-5}\gamma_{Dye}c_{H_2O_2} \\ & + 7.576 \times 10^{-4}c_{H_2O_2}\text{pH} + 1.401 \times 10^{-4}(c_{H_2O_2})^2 \\ & - 8.258 \times 10^{-3}(T)^2 \quad (10) \end{aligned}$$

$$\begin{aligned} \sqrt{\text{TOC}} = & 1.046 + 0.061\gamma_{Dye} - 2.958 \times 10^{-3}c_{H_2O_2} - 5.450 \times 10^{-3}t \\ & + 0.047\text{pH} - 2.708 \times 10^{-5}\gamma_{Dye}c_{H_2O_2} - 1.709 \times 10^{-4}(\gamma_{Dye})^2 \\ & + 2.601 \times 10^{-5}(c_{H_2O_2})^2 \quad (11) \end{aligned}$$

Eq. (12) is a simple mass balance equation through which the concentration of the dye in the diluted solution and the volume of the water to be added are calculated.

$$\gamma_{Dye}^i V^i = \gamma_{Dye} (V^i + V_{H_2O}) \quad (12)$$

Inequality Eq. (13) imposes a constraint on the number of times the reactor is loaded with the dye solution.

$$N_L \geq (V^i + V_{H_2O})/V_R \quad (13)$$

The inequality states that the number of reactor loadings ( $N_L$ ) must be greater or equal to the quotient between the total volume

**Table 2**  
Optimization results (CM formulation).

Run	Cost parameters		Optimal operating parameters							Cost
	$C_{H_2O_2}$ (€/L)	$C_E$ (€/kWh)	$T$ (°C)	$t^a$ (min)	pH (/)	$\gamma_{Dye}^b$ (mg/L)	$c_{H_2O_2}$ (mmol/L)	$V_{H_2O}$ (L)	$N_L$ (/)	$C_T$ (€/L)
1	0.5	0.05	35	31	6.1	80	184	0.0	1	0.017
2	1.0	0.05	35	70	7.1	40	14	1.8	2	0.021
3	1.5	0.05	35	72	6.9	40	12	1.8	2	0.022
4	0.5	0.07	35	31	6.0	80	185	0.0	1	0.019
5	1.0	0.07	35	70	7.2	40	15	1.8	2	0.028
6	1.5	0.07	35	71	7.1	40	14	1.8	2	0.029
7	0.5	0.09	35	30	5.9	80	186	0.0	1	0.022
8	1.0	0.09	35	31	6.1	80	183	0.0	1	0.032
9	1.5	0.09	35	70	7.2	40	14	1.8	2	0.035

<sup>a</sup> Treatment time for treating the total volume of diluted dye solution assuming batch operation.

<sup>b</sup> Dye concentration after dilution.

of the diluted dye solution ( $V^i + V_{H_2O}$ ) and the volume of the reactor. Clearly, the number of reactor loadings can only be an integer number. Thus, the variable  $N_L$  is defined as an integer variable. The first consequence of defining  $N_L$  as the integer variable is that the optimization problem (Eqs. (6)–(24)) corresponds to a mixed-integer nonlinear program (MINLP). But more importantly, the potential consequence that only the electricity cost (see Eq. (6)) is correlated through this integer variable must be discussed.

First, as stated above, the number of reactor loadings must be an integer number. On the other hand, the extent to which the reactor should be filled is not subjected to any constraint. Because of that, the volume of the diluted dye solution may not match a multiple of the reactor volume. If this is the case, the electricity cost for the treatment of the one batch in which the reactor is not fully filled is underestimated (see assumption “f”). Consequently, the total treatment costs are underestimated. However, if the volume of the diluted dye solution corresponds to a multiple of the reactor volume, the costs are calculated properly.

The responses are constrained through Eqs. (14)–(18). Due to constraint given by Eq. (14), a feasible solution must produce decoloration, measured at  $\lambda_{max}$  greater or equal to 99%. On the other hand, the constraints represented by Eqs. (15)–(18) enforce limits on spectral absorption coefficients and total organic carbon. With the exception of the limit on decoloration at peak wavelength, the limits on all the other responses were chosen according to the Slovenian environmental legislation.

$$\Delta A \geq 99 \quad (14)$$

$$SAC_{\lambda=436\text{ nm}} \leq 7 \quad (15)$$

$$SAC_{\lambda=525\text{ nm}} \leq 5 \quad (16)$$

$$SAC_{\lambda=620\text{ nm}} \leq 3 \quad (17)$$

$$TOC \leq 60 \quad (18)$$

The inequalities (Eqs. (19)–(23)) represent lower and upper bounds on operating parameters as defined in Table 1.

$$10 \leq t \leq 60 \quad (19)$$

$$5 \leq c_{H_2O_2} \leq 200 \quad (20)$$

$$10 \leq \gamma_{Dye} \leq 80 \quad (21)$$

$$5.5 \leq \text{pH} \leq 11 \quad (22)$$

$$20 \leq T \leq 35 \quad (23)$$

The upper and lower bound on water volume ( $V_{H_2O}$ ) is given by Eq. (24). The former was determined as such that, given an initial volume of the dye solution ( $V^i = 1.8$  L) and initial dye concentration  $\gamma_{Dye}^i = 80$  mg/L, the lower bound on the dye concentration can be

achieved by means of dilution (see Eq. (12)).

$$0 \leq V_{H_2O} \leq 12.6 \quad (24)$$

### 4.3. Optimization results (CM formulation)

The above model was coded in GAMS [28] and solved using DICOPT [29] as a MINLP solver. To illustrate how the cost parameters affect the optimal solution, the model was solved using nine different combinations of hydrogen peroxide and electricity prices. The price of water was considered constant ( $1.9$  €/m<sup>3</sup>) in all runs.

The results of the optimization are presented in Table 2. In the second and third columns, prices of hydrogen peroxide ( $w_{H_2O_2} = 30\%$ ) and electricity are given. The optimal operating parameters corresponding to the unique combination of these prices are given in the subsequent seven columns. In the last column, the total costs of treatment are reported.

Several important observations can be made on the basis of the results presented in Table 2. To begin with, the optimal temperature for the UV/H<sub>2</sub>O<sub>2</sub> treatment of the dye solution containing C. I. Reactive Blue 268 is found to be 35 °C for all the reported combinations of prices. This temperature corresponds to the upper bound of the temperature interval ( $T = 35$  °C) used in the experiments.

Unlike the temperature, all the rest of the operating parameters are affected by the changes in prices of hydrogen peroxide and electricity. Generally, a low price of hydrogen peroxide favors its higher concentration. On the other hand, higher prices of hydrogen peroxide tend to drive its concentration towards lower values. Analogous, a shorter treatment time is preferred in case of higher electricity prices. This effect is especially notable when comparing the results at the price of hydrogen peroxide set to 1.0 €/L. A drastic decrease in total treatment time from 70 min to approximately 30 min is observed as electricity price is set to its highest value. To avoid any misinterpretations, it must be pointed out here that these observations should be considered as partial. The reader should be aware that the optimal values of operating parameters are determined in such a way that the total treatment costs are minimized. Therefore, not only the electricity price affects the treatment time, but also the price of hydrogen peroxide affects its concentration.

Another important operating parameter is the initial concentration of the dye that is manipulated by the dilution of the initial dye solution. As seen from the results, dilution is frequently utilized as a means to adjust the initial dye concentration. Whether or not water is being utilized is determined by the outcome of two conflicting factors. First, the dilution of the initial dye solution increases electricity costs due to the increase in the number of batches to be treated, and additional costs associated with water consumption. Second, the dilution enables efficient enough operation of the

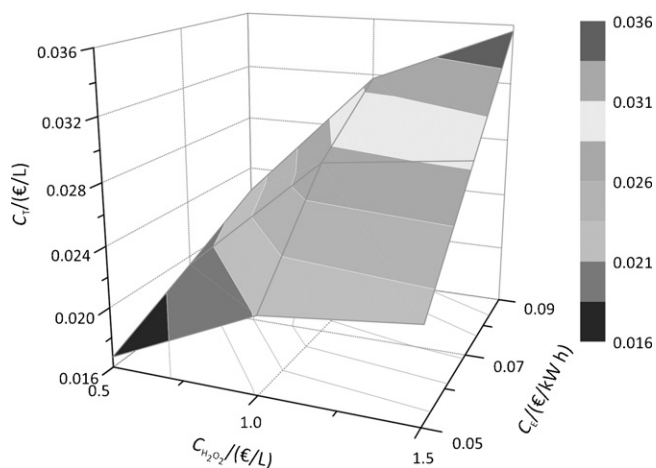


Fig. 4. Treatment costs as a function of electricity and hydrogen peroxide prices.

treatment process at lower  $\text{H}_2\text{O}_2$  concentrations, potentially reducing costs.

As a final point in this section, the total treatment costs are discussed. As intuitively expected, the total treatment costs increase with increasing prices of electricity and hydrogen peroxide. However, Fig. 4 shows that they do not increase linearly with linear increases in either electricity or hydrogen peroxide prices. This makes the task to determine or predict the minimal operating cost as a function of these prices somewhat difficult, unless proper methods are used. Using the proposed approach (CM formulation), the total treatment costs of the nine runs presented in Table 2 were determined to be in the range from 0.017 €/L to 0.035 €/L.

#### 4.4. Optimization results (CM formulation vs. RM formulation)

To compare the results of the proposed approach with the results obtained using maximization of the responses, the RM formulation of the model was solved. The mathematical program in accordance to RM formulation (see Eq. (2)) is not explicitly documented in this paper as there are only two differences with respect to the one presented in Section 4.2 (Eqs. (6)–(24)). These are:

The objective function (Eq. (6)) is replaced by Eq. (25). Note that the value of the objective variable  $R$  is at its maximum when  $\Delta A$  is at its attainable maximum value, and SACs and TOC at their attainable minimum values.

$$\max R = \Delta A - \text{SAC}_{\lambda=436\text{ nm}} - \text{SAC}_{\lambda=525\text{ nm}} - \text{SAC}_{\lambda=620\text{ nm}} - \text{TOC} \quad (25)$$

The constraints given by Eqs. (12)–(18) are redundant.

Table 3  
Optimization results (RM formulation).

Run	Cost parameters		Optimal operating conditions							Cost $C_T^c$ (€/L)
	$C_{\text{H}_2\text{O}_2}$ (€/L)	$C_E$ (€/kWh)	$T$ (°C)	$t^a$ (min)	pH (/)	$\gamma_{\text{dye}}^b$ (mg/L)	$C_{\text{H}_2\text{O}_2}$ (mmol/L)	$V_{\text{H}_2\text{O}}$ (L)	$N_L^c$	
1	0.5	0.05								0.078
2	1.0	0.05								0.096
3	1.5	0.05								0.113
4	0.5	0.07								0.100
5	1.0	0.07	35	240	5.5	23	98	4.5	4	0.118
6	1.5	0.07								0.135
7	0.5	0.09								0.122
8	1.0	0.09								0.140
9	1.5	0.09								0.158

<sup>a</sup> Treatment time for treating the total volume of diluted dye solution assuming batch operation.

<sup>b</sup> Dye concentration after dilution.

<sup>c</sup> Post-processing calculations.

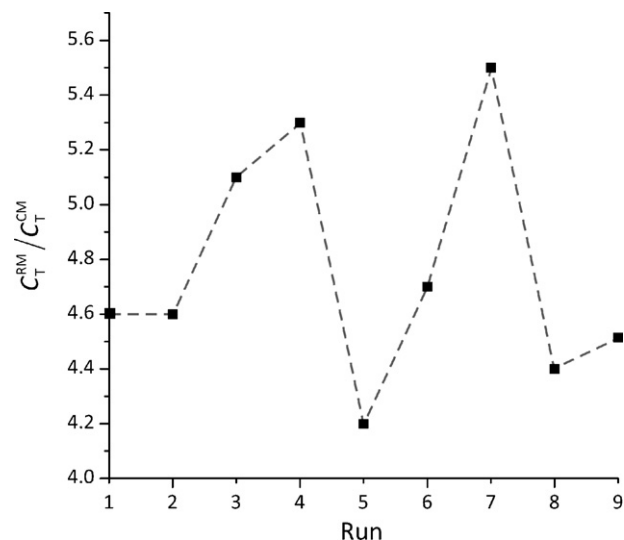
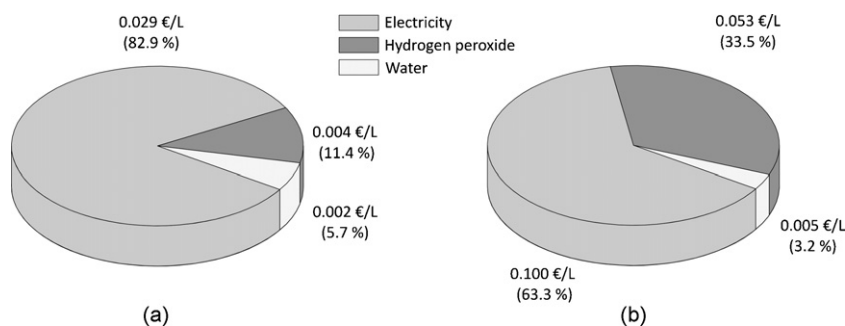


Fig. 5. Cost ratios.

The results of the optimization based on the RM formulation are presented in Table 3. Although the RM formulation does not contain any cost terms, the treatment costs are reported. Also reported are the volumes of water needed to adjust the dye concentration, and number of reactor loadings. Note that these quantities are not a part of the optimization problem. Their values were calculated afterwards on the basis of the obtained optimal operating conditions. For the calculation of treatment costs, the same cost terms given in Eq. (6) were used.

Also important to note is that, because the objective function in RM is just a sum of the responses; the same values of operating conditions are guaranteed regardless of the presumable prices of electricity, hydrogen peroxide, and water. In the following paragraphs, the most notable differences among the results obtained using the CM and RM formulations are discussed.

With the exception of the optimal operating temperature, which is found to be the same in all the runs (Tables 2 and 3), relatively large differences in values of all the other operating parameters are observed. The operating parameter not discussed so far is pH. As denoted in Section 3.2, the UV/ $\text{H}_2\text{O}_2$  oxidation technology is most efficient under neutral to weakly acidic conditions. The results presented in Tables 2 and 3 are in agreement with these findings. However, an important difference among the results obtained using the two formulations is that the optimal pH determined by the RM formulation is at a lower bound of the experimental pH region (pH 5.5). Because the solution is at its bound, this may be an indication that the limits on pH are too tight, and the true optimal solution,



**Fig. 6.** (a) Distribution of costs in a solution of CM formulation ( $C_{H_2O_2} = 1.5 \text{ €/L}$ ,  $C_E = 0.09 \text{ €/kWh}$ ,  $C_{H_2O} = 0.002 \text{ €/L}$ ). (b) Distribution of costs in a solution of RM formulation ( $C_{H_2O_2} = 1.5 \text{ €/L}$ ,  $C_E = 0.09 \text{ €/kWh}$ ,  $C_{H_2O} = 0.002 \text{ €/L}$ ).

from the perspective of process efficiency, lies outside the experimental region. On the other hand, the optimal pH values found using the CM formulation are well within the bounds of the experimental region. Depending on the prices of hydrogen peroxide and electricity, the optimal pH ranges from 5.9 to 7.2.

Another major difference observed is the optimal initial concentration of  $H_2O_2$ . For the RM formulation, its optimal concentration is found to be 98 mmol/L. It is interesting to note that, although no costs are associated with the consumption of hydrogen peroxide, its concentration does not reach the upper limit (200 mmol/L). Again, this result is in agreement with the findings in the literature [30,31], where it is reported that either too low or too high concentrations of  $H_2O_2$  reduce the efficiency of the oxidation process.

Perhaps the most obvious differences are those in the treatment costs. From the inspection of the values reported in Tables 2 and 3, it is clear that the solutions obtained using the CM formulation are, from the economical point of view, superior to those obtained using the RM formulation. Additional confirmation of the foregoing statement is given by the cost ratios depicted in Fig. 5.

The lowest ratio observed is 4.2 (run 5), while the highest ratio is 5.5 (run 7), all favoring the solutions obtained using the CM formulation. From a slightly different perspective, even the highest treatment cost reported in Table 2 is still approximately two times

lower than the lowest treatment cost reported in Table 3. Clearly, achieving the attainable extreme values of the responses has its price.

The highest total treatment costs observed for the two optimization approaches were 0.035 €/L (Table 2) and 0.158 €/L (Table 3), corresponding to the highest price of hydrogen peroxide and electricity. For illustrative purpose, these two solutions were selected to present the contribution of the individual costs to the total treatment cost (Fig. 6).

In both cases, the electricity cost represents by far the greatest fraction (>60%) of the total operating cost. Similar percent contributions of electricity cost to total operating cost can also be calculated for all the other runs presented in Table 2, suggesting that the efficiency of the UV radiation source represents a bottleneck for additional improvements in economic efficiency of the treatment process.

Percent contribution of electricity cost is followed by percent contribution of hydrogen peroxide cost. The latter represents roughly 34% of total operating costs in case when the treatment was optimized solely from the perspective of treatment efficiency (Fig. 6b). On the other hand, hydrogen peroxide cost represents around 11% of total treatment cost when the process performance was optimized simultaneously with all the relevant treatment costs (Fig. 6a). The lowest percent contribution to total treatment costs

**Table 4**

Predicted and experimentally determined values of the responses. CM formulation (runs 1–9) and RM formulation (run 10).

Run	$\Delta A$ (%)	$SAC_{\lambda=436 \text{ nm}}$ ( $\text{m}^{-1}$ )	$SAC_{\lambda=525 \text{ nm}}$ ( $\text{m}^{-1}$ )	$SAC_{\lambda=620 \text{ nm}}$ ( $\text{m}^{-1}$ )	$\Delta TOC$ (%)
1	99.0 <b>99.2</b>	6.3 <b>5.1</b>	2.8 <b>2.7</b>	3.0 <b>2.8</b>	15 <b>16</b>
2	99.0 <b>98.9</b>	2.8 <b>3.1</b>	1.8 <b>2.2</b>	3.0 <b>3.1</b>	60 <b>62</b>
3	99.0 <b>98.8</b>	2.8 <b>3.7</b>	1.8 <b>2.1</b>	3.0 <b>3.2</b>	61 <b>57</b>
4	99.0 <b>99.3</b>	6.5 <b>5.0</b>	2.9 <b>2.5</b>	3.0 <b>2.7</b>	15 <b>14</b>
5	99.0 <b>99.0</b>	2.8 <b>2.9</b>	1.8 <b>2.2</b>	3.0 <b>3.0</b>	61 <b>64</b>
6	99.0 <b>99.1</b>	2.9 <b>3.0</b>	1.8 <b>2.0</b>	3.0 <b>2.9</b>	61 <b>62</b>
7	99.0 <b>98.7</b>	6.7 <b>6.2</b>	3.0 <b>3.4</b>	3.0 <b>3.2</b>	14 <b>13</b>
8	99.0 <b>99.0</b>	6.2 <b>5.2</b>	2.9 <b>2.6</b>	3.0 <b>3.0</b>	15 <b>17</b>
9	99.0 <b>99.2</b>	2.8 <b>2.3</b>	1.8 <b>1.9</b>	3.0 <b>2.8</b>	60 <b>63</b>
10	100.0 <b>99.9</b>	0.09 <b>0.2</b>	0.03 <b>0.1</b>	0.0 <b>0.1</b>	91 <b>94</b>

Experimentally determined values are typed in bold.

**Table 5**

Gamma correlation coefficients.

	Experimental				
	$\Delta A$ (%)	$SAC_{\lambda=436 \text{ nm}}$ ( $\text{m}^{-1}$ )	$SAC_{\lambda=525 \text{ nm}}$ ( $\text{m}^{-1}$ )	$SAC_{\lambda=620 \text{ nm}}$ ( $\text{m}^{-1}$ )	$\Delta TOC$ (%)
Predicted					
$\Delta A$ (%)	1.000				
$SAC_{\lambda=436 \text{ nm}}$ ( $\text{m}^{-1}$ )		0.744			
$SAC_{\lambda=525 \text{ nm}}$ ( $\text{m}^{-1}$ )			0.882		
$SAC_{\lambda=620 \text{ nm}}$ ( $\text{m}^{-1}$ )				1.000	
$\Delta TOC$ (%)					0.838

Correlations are significant at  $p < 0.05$ .



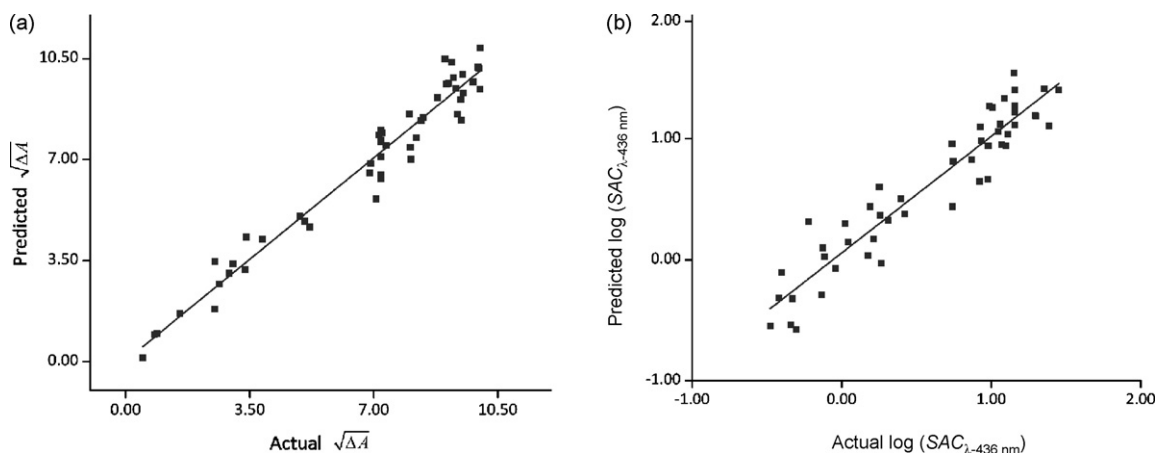


Fig. 7. Actual vs. predicted plots: (a) percent decoloration at  $\lambda_{\max} = 634$  nm; (b) spectral absorption coefficient at  $\lambda = 463$  nm.

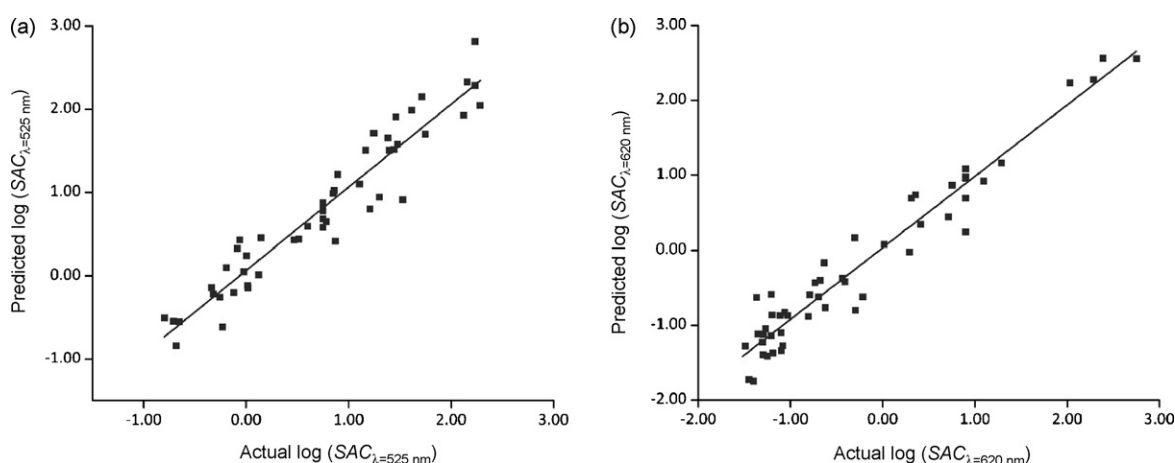


Fig. 8. Actual vs. predicted plots: (a) spectral absorption coefficient at  $\lambda = 525$  nm; (b) spectral absorption coefficient at  $\lambda = 620$  nm.

corresponds to the cost of water. The latter is found to be less than 6% in both cases.

However, when comparing absolute values of hydrogen peroxide cost (Fig. 6a) and water cost (Fig. 6b), it can be seen that the cost of water exceeds the cost of hydrogen peroxide. This confirms the need that the cost of water, if used for diluting the initial dye solution, should be taken into account when optimizing or assessing the acceptability of the UV/H<sub>2</sub>O<sub>2</sub> treatment technology.

#### 4.5. Evaluation of solutions

To evaluate the quality of the solutions obtained by the two formulations a series of experiments was performed. The operating conditions (initial dye and hydrogen peroxide concentration, pH, treatment time, and temperature) corresponded to the ones shown in Tables 2 and 3. The values of the responses determined by optimization of the H<sub>2</sub>O<sub>2</sub>/UV treatment process (predictions), and the values of responses determined experimentally (observations) are shown in Table 4.

**Table 6**  
Statistics for the quadratic models.

Model	$\Delta A$	$SAC_{\lambda=436 \text{ nm}}$	$SAC_{\lambda=525 \text{ nm}}$	$SAC_{\lambda=620 \text{ nm}}$	TOC
$R^2$	0.95	0.87	0.90	0.93	0.97
$R^2_{\text{adj}}$	0.93	0.86	0.90	0.92	0.97
$R^2_{\text{pred}}$	0.92	0.85	0.89	0.90	0.96

To quantitatively assess the degree of correlation among the predictions and observations, the gamma statistics, belonging to a group of nonparametric statistical methods, was used. The gamma statistics is preferred over some other nonparametric association/correlation statistical methods (i.e. Spearman's  $r$ , Kendall's  $\tau$ ) in cases when a set of data contains many ties. It should be noted that nonparametric statistical methods are a somewhat less powerful than parametric ones if the assumptions underlying the latter

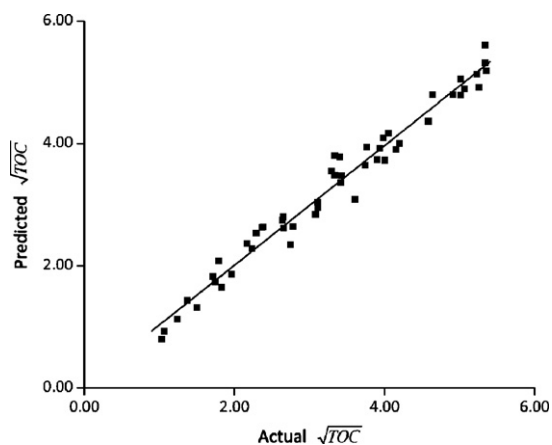


Fig. 9. Actual vs. predicted plot: total organic carbon.

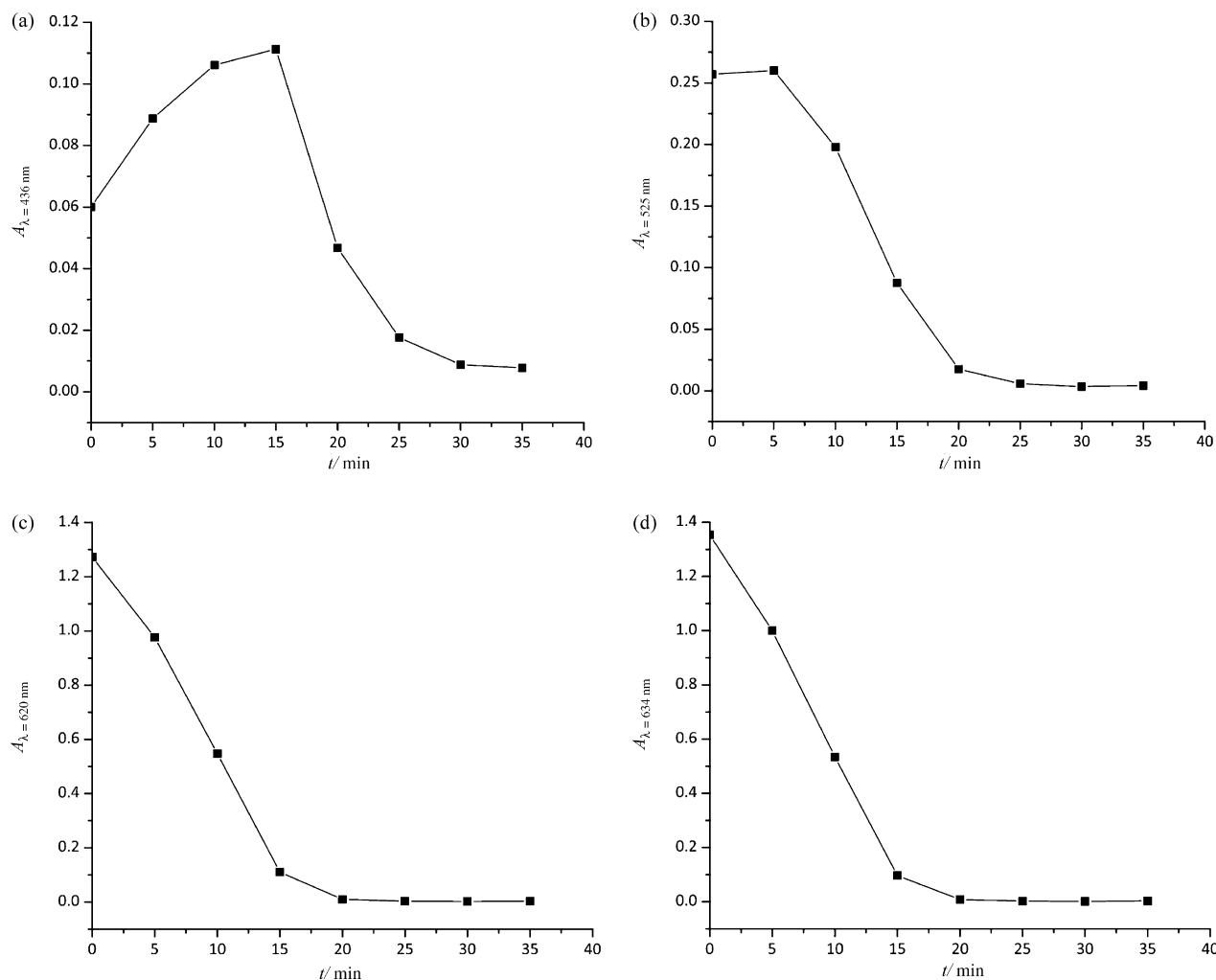


Fig. 10. Change in absorbance at different wavelengths as a function of time (experimental conditions:  $\gamma_{\text{Dye}} = 45 \text{ mg/L}$ ,  $c_{\text{H}_2\text{O}_2} = 102.5 \text{ mmol/L}$ , pH 8.25,  $T = 27.5^\circ \text{C}$ ).

are met, however, they are less likely to give distorted results when those assumptions fail [32].

From the results given in Table 5 we can establish that there is a strong positive correlation ( $J_{\text{Pred., Exp.}}^{\text{min}} > 0.74$ ) among the predicted and experimentally determined values of the responses. According to this criterion, we can establish that the predicted values are in good agreement with the experimentally measured ones.

## 5. Conclusions

In this paper, the decoloration and mineralization of wastewater containing C. I. Reactive Blue 268 dye using UV/ $\text{H}_2\text{O}_2$  treatment technology was investigated. Particular emphasis was given to developing an optimization procedure through which the treatment technology was simultaneously optimized from the perspective of operating and economic efficiency. The presented approach is based on a response surface methodology in conjunction with mathematical programming.

The results indicate that if the simultaneous optimization of operating parameters and costs is used, a significant improvement in economic efficiency of the treatment technology can be achieved. For the case studied, the operating cost of the treatment process optimized solely with respect to the maximization of operating efficiency could be up to 5.5 times higher than those obtained using the proposed approach.

In summary, to fully explore the potentials of UV/ $\text{H}_2\text{O}_2$  treatment technology or, for that matter, any kind of technology, the operating cost should be considered as an integral part of the optimization process whenever applicable.

## Acknowledgements

Nina Novak is grateful to the Ministry of Higher Education, Science and Technology of the Republic of Slovenia and Tekstina d. d. Ajdovščina (Contract: 321-05-000-565).

## Appendix A

Plots of actual responses vs. those predicted by the quadratic polynomial approximations (Eqs. (7)–(11)) are depicted in Figs. 7–9.

Additional statistics for the quadratic polynomial approximations presented in Section 4.2 are given in Table 6. In all cases,  $R_{\text{pred}}^2$  was in reasonable agreement with  $R_{\text{adj}}^2$ . In addition, signal to noise ratio (SN) was adequate ( $\text{SN} > 4$ ). Lack of fit was statistically insignificant.  $F$ -values implied that the models are statistically significant. The insignificant terms were excluded using the backward elimination procedure.

Slightly lower values of  $R^2$ ,  $R_{\text{adj}}^2$ , and  $R_{\text{pred}}^2$  were observed in the case of the  $\text{SAC}_{\lambda=436 \text{ nm}}$  polynomial model. This could be ascribed to the fact that the absorbance at  $\lambda = 436 \text{ nm}$  increases during the

first 15 min of the UV/H<sub>2</sub>O<sub>2</sub> treatment (Fig. 10a), and only after that decreases. This highly nonlinear behavior could cause potential difficulties in fitting.

Plots in Fig. 10 also confirm the need to monitor the decoloration process at multiple wavelengths. Reasonable (desired) decoloration at  $\lambda_{\max}$  may not be sufficient because the absorbance does not necessarily decrease monotonically on the entire visible spectra.

## References

- [1] H. Suty, C. De Traversay, M. Cost, Applications of advanced oxidation processes: present and future, *Water Sci. Technol.* 49 (2004) 227–233.
- [2] H.-Y. Shu, M.-C. Chang, Decolorization effects of six azo dyes by O<sub>3</sub>, UV/O<sub>3</sub> and UV/H<sub>2</sub>O<sub>2</sub> processes, *Dyes Pigm.* 65 (2005) 25–31.
- [3] I. Muthuvel, M. Swaminathan, Photoassisted Fenton mineralisation of Acid Violet 7 by heterogeneous Fe(III)–Al<sub>2</sub>O<sub>3</sub> catalyst, *Catal. Commun.* 8 (2007) 981–986.
- [4] S. Vajnhandl, A. Majcen Le Marechal, Case study of the sonochemical decoloration of textile azo dye Reactive Black 5, *J. Hazard. Mater.* 141 (2007) 329–335.
- [5] E.R. Bandala, M.A. Peláez, A.J. García-López, M. de, J. Salgado, G. Moeller, Photocatalytic decolorisation of synthetic and real textile wastewater containing benzidine-based azo dyes, *Chem. Eng. Process* 47 (2008) 169–176.
- [6] S. Parsons, *Advanced Oxidation Processes for Water and Wastewater Treatment*, IWA Publishing, London, UK, 2004, pp. 101–103.
- [7] F.H. Abdullah, M.A. Rauf, A.S.S. Ashraf, Kinetics and optimization of photolytic decoloration of carmine by UV/H<sub>2</sub>O<sub>2</sub>, *Dyes Pigm.* 75 (2007) 194–198.
- [8] H.-Y. Shu, M.-C. Chang, H.-J. Fan, Decolorization of azo dye acid black 1 by the UV/H<sub>2</sub>O<sub>2</sub> process and optimization of operating parameters, *J. Hazard. Mater.* 113 (2004) 201–208.
- [9] O.L.C. Guimarães, D.N.V. Filho, A.F. Siqueira, H.J.I. Filho, M.B. Silva, Optimization of the azo dyes decoloration process through neural networks: determination of the H<sub>2</sub>O<sub>2</sub> addition critical point, *Chem. Eng. J.* 141 (2008) 35–41.
- [10] B.K. Körbahti, M.A. Rauf, Application of response surface analysis to the photolytic degradation of Basic Red 2 dye, *Chem. Eng. J.* 138 (2008) 166–171.
- [11] M.A. Rauf, N. Marzouki, B.K. Körbahti, Photolytic decolorization of Rose Bengal by UV/H<sub>2</sub>O<sub>2</sub> and data optimization using response surface method, *J. Hazard. Mater.* 159 (2008) 602–609.
- [12] J. Fernández, J. Kiwi, C. Lizama, J. Freer, J. Baeza, H.D. Mansilla, Factorial experimental design of Orange II photocatalytic discoloration, *J. Photochem. Photobiol. A* 151 (2002) 213–219.
- [13] I.-H. Cho, K.-D. Zoh, Photocatalytic degradation of azo dye (Reactive Red 120) in TiO<sub>2</sub>/UV system: optimization and modeling using a response surface methodology (RSM) based on the central composite design, *Dyes Pigm.* 75 (2007) 533–534.
- [14] S. Hammami, N. Oturan, N. Bellakhal, M. Dachraoui, M.A. Oturan, Oxidative degradation of direct orange 61 by electro-Fenton process using a carbon felt electrode: application of the experimental design methodology, *J. Electroanal. Chem.* 610 (2007) 75–84.
- [15] K. Hunger, *Industrial Dyes, Chemistry Properties, Applications*, vol. 353, Wiley VCH, Weinheim, Germany, 2003, p. 112.
- [16] T. Hihara, Y. Okada, Z. Morita, The reaction of triphenyldioxazine dyes with bleaching agents, hypochlorite and hydrogen peroxide, in aqueous solution, *Dyes Pigm.* 46 (2000) 181–192.
- [17] R.H. Myers, D.C. Montgomery, *Response Surface Methodology, Process and Product Optimization Using Designed Experiments*, 2nd ed., John Wiley and Sons, New York, 2002, p. 235.
- [18] S.J. Sadjadi, M. Habibian, V. Khaledi, A multi-objective decision making approach for solving quadratic multiple response surface problems, *Int. J. Contemp. Math. Sci.* 3 (2008) 1595–1606.
- [19] L. Wei, Y. Yuying, Multi-objective optimization of sheet metal forming process using Pareto-based genetic algorithm, *J. Mater. Process. Technol.* 208 (2008) 499–506.
- [20] K.M. Miettinen, *Nonlinear Multiobjective Optimization*, Kluwer Academic Publishers, Boston, USA, 1999.
- [21] I. Nicole, J. De Laat, M. Dore, J.P. Duguet, C. Bonnel, Use of UV radiation in water treatment: measurement of photonic flux by hydrogen peroxide actinometry, *Water Res.* 24 (1990) 157–168.
- [22] D. VanOsdell, K. Foarde, Defining the effectiveness of UV lamps installed in circulating air ductwork, Report ARTI-21CR/610-40030-01, Air-Conditioning and Refrigeration Technology Institute, Arlington, Virginia, USA, 2002, <http://www.osti.gov/bridge/servlets/purl/810964-SRS2Dd/native/810964.PDF>.
- [23] W.Z. Tang, *Physicochemical Treatment of Hazardous Wastes*, Lewis Publishers, Boca Raton, Florida, 2004, p. 271.
- [24] H.-Y. Shu, M.-C. Chang, Development of a rate expression for predicting decolorization of C.I. Acid Black 1 in a UV/H<sub>2</sub>O<sub>2</sub> process, *Dyes Pigm.* 70 (2006) 31–37.
- [25] Integrated Pollution Prevention and Control (IPPC), Reference document on best available techniques for the textiles industry, 2003, BREF (07.03), pp. 320–321, <http://www.eippcb.jrc.ec.europa.eu/pages/FActivities.htm>.
- [26] A. Gottlieb, C. Shaw, A. Smith, A. Wheatley, S. Forsythe, The toxicity of textile reactive azo dyes after hydrolysis and decolorisation, *J. Biotechnol.* 101 (2003) 49–56.
- [27] Ur. I. RS 7/2007: Decree on the emission of substances in the discharge of waste water from plants and facilities for the production, processing and working of textile fibres (Uredba o emisiji snovi in toplote pri odvajanju odpadne vode iz naprav za proizvodnjo, predelavo in obdelavo tekstilnih vlaken), <http://www.uradni-list.si/1/objava.jsp?urlid=20077&stevilka=239>.
- [28] R.E. Rosenthal, *GAMS – A User's Guide*, GAMS Development Corporation, Washington, DC, 2007, [www.gams.com](http://www.gams.com).
- [29] J. Viswanathan, I.E. Grossmann, A combined penalty function and outer approximation method for MINLP optimization, *Comput. Chem. Eng.* 14 (1990) 769–782.
- [30] I. Peternel, N. Koprivanac, H. Kusic, UV-based process for reactive dye mineralization, *Water Res.* 40 (2006) 525–532.
- [31] B.K. Körbahti, M.A. Rauf, Determination of optimum operating conditions of carmine decoloration by UV/H<sub>2</sub>O<sub>2</sub> using response surface methodology, *J. Hazard. Mater.* 161 (2009) 281–286.
- [32] D.J. Sheskin, *Handbook of Parametric and Nonparametric Statistical Procedures*, 3rd ed., Chapman & Hall/CRC, Boca Raton, USA, 2004, pp. 1108–1122.